J. Membrane Biol. 94, 173–190 (1986)

The Journal of
Membrane Biology

Membrane Potentials and Intracellular Cl^- Activity of Toad Skin Epithelium in Relation to Activation and Deactivation of the Transepithelial Cl^- Conductance

N.J. Willumsen* and E. Hviid Larsen

Institute of Medical Physiology, Dept. A, The Panum Institute, University of Copenhagen, 2200 Copenhagen N, Denmark, and Zoophysiological Laboratory A, The August Krogh Institute, University of Copenhagen, 2100 Copenhagen Ø, Denmark

Summary. The potential dependence of unidirectional ^{36}Cl fluxes through toad skin revealed activation of a conductive pathway in the physiological region of transepithelial potentials. Activation of the conductance was dependent on the presence of Cl^- or Br^- in the external bathing solution, but was independent of whether the external bath was NaCl-Ringer's, NaCl-Ringer's with amiloride, KCl-Ringer's or choline Cl-Ringer's. To partition the routes of the conductive Cl^- ion flow, we measured in the isolated epithelium with double-barrelled microelectrodes apical membrane potential, V_a, and intracellular Cl^- activity, a^c_{Cl}, of the principal cells identified by differential interference contrast microscopy. Under short-circuit conditions, I_{sc} = 27.0 ± 2.0 μA/cm², with NaCl-Ringer's bathing both surfaces, V_a was −67.9 ± 3.8 mV (mean ± SE, n = 24, six preparations) and a^c_{Cl} was 18.0 ± 0.9 mM in skins from animals adapted to distilled water. Both V_a and a^c_{Cl} were found to be positively correlated with I_{sc} (r = 0.66 and r = 0.70, respectively). In eight epithelia from animals adapted to dry milieu/tap water V_a and a^c_{Cl} were measured with KCl Ringer's on the outside during activation and deactivation of the transepithelial Cl^- conductance (G_{Cl}) by voltage clamping the transepithelial potential (V) at 40 mV (mucosa positive) and −100 mV. At V = 40 mV; i.e. when G_{Cl} was deactivated, V_a was −70.1 ± 5.0 mV (n = 15, eight preparations) and a^c_{Cl} was 40.0 ± 3.8 mM. The fractional apical membrane resistance (fR_a) was 0.69 ± 0.03. Clamping to V = −100 mV led to an instantaneous change of V_a to 31.3 ± 5.6 mV (cell interior positive with respect to the mucosal bath), whereas neither a^c_{Cl} nor fR_a changed significantly within a 2 to 5-min period during which G_{Cl} increased by 1.19 ± 0.10 mS/cm². When V was stepped back to 40 mV, V_a instantaneously shifted to −67.8 ± 3.9 mV while a^c_{Cl} and fR_a remained constant during deactivation of G_{Cl}. Similar results were obtained in epithelia impaled from the serosal side. In 12 skins from animals adapted to either tap water or distilled water the density of mitochondria-rich (D_{MRC}) cells was estimated and correlated with the Cl current (I_{Cl} through the fully activated (V = −100 mV) Cl^- conductance). A highly significant correlation was revealed (r = −0.96) with a slope of −2.6 nA/m.r. (mitochondria-rich cell and an I-axis intercept not significantly different from zero. In summary, the voltage-dependent Cl currents were not reflected in fR_a and a^c_{Cl} of the principal cells but showed a correlation with the m.r. cell density. We conclude that the principal cells do not contribute significantly to the voltage-dependent Cl conductance.

Key Words toad skin epithelium · voltage-clamp currents · membrane potential · intracellular Cl^- activity · voltage-dependent Cl^- conductance · mitochondria-rich cells

Introduction

Passive transepithelial Cl^- fluxes of toad (*Bufo bufo*) skin exhibit a complex voltage-dependence owing to a gated Cl^- permeability that is turned on over the range of physiological potentials (mucosa negative) and turned off at potentials above 0 mV. As a result, the steady-state conductive Cl^- ion flow is large only when its electric driving force is inwardly directed, whereas the net flux of Cl^- becomes virtually zero when the driving force is reversed (Larsen & Kristensen, 1978; Larsen & Rasmussen, 1982).

As the magnitude of passive Cl^- fluxes in the short-circuited frog skin decreases when the active Na^+ flux is reduced (Macey & Meyers, 1963; Candia, 1978; Kristensen, 1978; Ques-von Petery et al., 1978), the Cl^- permeability was suggested to reside in a major Na^+-transporting compartment, i.e. the principal cells[1] of the epithelium. However, results published recently by others are difficult to reconcile with the passage of large dissipative Cl^- fluxes through these cells. For example, under short-circuit conditions a low Cl^- permeability of the outer epithelial barrier (Nagel, 1977; Ferreira & Ferreira, 1981; Nagel et al., 1981; Stoddard & Helman, 1982; Giraldez & Ferreira, 1984; Biber et al., 1985) and an intracellular Cl^- activity far above equilibrium (Rick et al., 1978; Nagel et al., 1981; Giraldez & Ferreira, 1984; Harvey & Kernan, 1984; Biber et al., 1985) have been reported. Furthermore, Voûte and Meier (1978), Kristensen (1981) and Katz and Larsen (1984) presented evidence that the trans-

* *Present address:* Division of Pulmonary Diseases, 724 Burnett-Womack Bldg. 299H, University of North Carolina, Chapel Hill, NC 27514.

[1] Principal cells denotes the major population of epithelial cells located from the stratum germinativum to the stratum granulosum, excluding the m.r. cells.

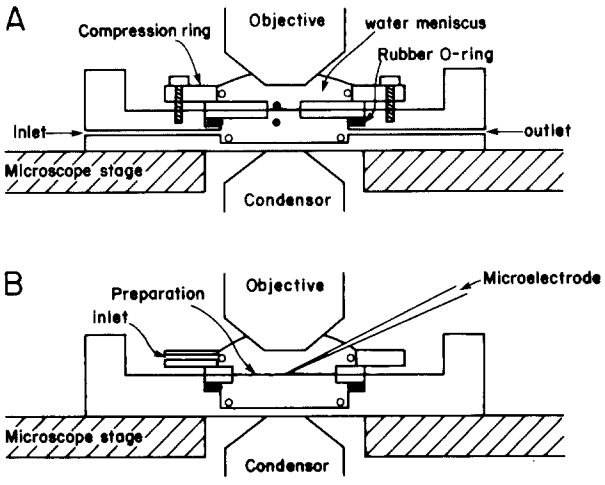

Fig. 1. Experimental chamber for microelectrode measurements in identified cells of isolated epithelia. Panels *A* and *B* show perpendicular cross-sections illustrating the rectangular positions of electrodes, perfusion tubes, and the exposed epithelial area. The Figure is not drawn to scale

epithelial Cl^- pathway in the frog or toad skin is localized to the mitochondria rich (m.r.) cells. Because these cells do not take part in the functional syncytium made up by the more numerous principal cells (Rick et al., 1978), the dependence of the Cl^- fluxes on the active Na^+ flux suggests that at least a small component of the active Na^+ flux passes the m.r. cells. This view is supported by the finding that excretion of the vital dye, methylene blue, by the m.r. cells is inhibited by amiloride and ouabain (Ehrenfeld et al., 1976), which are specific blockers of active Na^+ transport in high-resistance epithelia. Also it is in agreement with the finding that the Na^+ gain by m.r. cells following ouabain treatment of frog skin was partially prevented by exposure of the outer border of the skin to amiloride (Rick et al., 1978).

In the present study we investigated the conductive Cl^- permeability of the principal cells of toad skin. This was done by measurements of membrane potentials and the intracellular Cl^- activity of these cells in response to voltage activation and deactivation of the transepithelial Cl^- conductance. We also determined the relationship between the density of the mitochondria-rich cells, and the fully activated potential-dependent Cl^- conductance. Thus, the experiments to be presented extend previous tracer flux (Ferreira & Ferreira, 1981; Stoddard & Helman, 1982) and microelectrode (Nagel et al., 1981; Harvey & Kernan, 1984; Biber et al., 1985) studies of the short-circuited frog skin by taking in account that at $V = 0$ mV the conductive Cl^- permeability is very low, but that the Cl^- conductance reversibly can be turned fully on by clamping the tissue at $V \leq -80$ mV.

Part of this study have been published elsewhere (Willumsen & Larsen, 1984, 1985*a*,*b*).

Materials and Methods

Preparation

The epidermis of the belly skin, isolated in the intermoult period, was obtained from the common European toad (*Bufo bufo*). The majority of experiments to be reported were carried out with animals kept on filter paper with free access to tap water and given mealworms *ad libitum*, i.e. under conditions mimicking the natural habitat of this terrestrial species.

In contrast to animals kept under the above conditions, skin of animals kept in distilled water generally exhibit larger, more variable short-circuit currents. Thus, for the initial studies on membrane potentials and intracellular Cl^- activities, we used animals kept in distilled water (8 to 12 days), to compare our measurements with those reported in the literature from frog skins generating similar large and variable short-circuit currents.

The epithelium was isolated by exposing the serosal side of the skin to a 0.25 mg/ml collagenase solution (103586, Boehringer Mannheim GmbH) for 2 to 3 hr. After this treatment the intact epithelium was removed from the partly digested corium and stored at 5°C in NaCl-Ringer's containing 5 mM acetate.

Experimental Chamber

The isolated epithelium was mounted in a mini Ussing-chamber with a slit-shaped exposed area of 2 × 5 mm (Fig. 1). The serosal and the mucosal half-chambers, that could be perfused continuously, contained a pair of Ag/AgCl electrodes for potential recording and current passing, respectively. These were connected to a voltage-clamp circuit providing fast (msec) voltage clamping of the preparation between −200 and +200 mV. The chamber was placed directly on a microscope stage, and the impalements were visually inspected at 400× magnification by differential interference contrast (DIC, Nomarski) microscopy employing a Zeiss 40/0.75 water immersion objective with a working distance of 1.6 mm.

Ringer's Solutions

The composition of the employed Ringer's solution was:

NaCl-Ringer's (mM): 114.4 Na^+, 2.4 K^+, 1.0 Ca^{2+}, 116.4 Cl^-, 2.4 HCO_3^-, pH = 8.2 following bubbling with atmospheric air. To the NaCl-Ringer's bathing the serosal side was added 5 mM Na-acetate.

KCl-Ringer's: Na^+ substituted by K^+. Otherwise identical to NaCl-Ringer's.

Na-gluconate-Ringer's: Cl^- substituted by gluconate. Otherwise identical to NaCl-Ringer's.

Microelectrodes

Double-barrelled Cl^--selective microelectrodes were constructed according to the technique of Zeuthen et al. (1974) from

1.2 mm OD glass capillary (Corning 120F) for the reference barrel and 1.8 mm OD glass capillary (Jencons) for the ion-selective barrel. The nitric acid-washed capillaries were glued together with an epoxy glue (Araldit) heated and twisted 360°, and pulled on a horizontal puller (Narishige, model PD-5). The tip diameter of the electrode was less than 1 μm. The ion-selective barrel was silanized (dichlorodimethylsilane) for 5 to 10 sec and heated for 1 hr at 100°C before filling the tip with Cl^- ion exchanger (Corning 477913). Finally, the ion-selective barrel was backfilled with 0.5 or 2 M KCl. The reference barrel was backfilled with either 0.5 M Na_2SO_4 or 0.5 M KCl, or the tip was filled with 0.5 M Na_2SO_4 whereas the stem of the electrode was filled with 2 M KCl. The estimated Cl^- activities were independent of the electrolyte composition of the reference barrel, indicating that leakage of Cl^- from the reference barrel was insignificant. Heating of the electrode was found to impair the selectivity and slow the response time of the ion exchanger. Therefore, air bubbles, if present, were removed by thin glass filaments. When filled with 2 M KCl, the resistance of the reference barrel was 30 to 100 Mohm. The electrodes were calibrated in KCl solutions of either variable (0.01, 0.03 and 0.1 M KCl) or constant (0.01 M KCl + 0.09 M Na-gluconate, 0.03 M KCl + 0.07 M Na-gluconate and 0.1 M KCl) ionic strength. In both cases, the sensitivity (S) ranged from 50 to 59 mV per decalog Cl^- activity, with $S = 57.4 \pm 0.5$ mV/decalog for 16 randomly selected electrodes. The HCO_3^-/Cl^- selectivity coefficient was 0.11 ± 0.01 ($n = 16$). As a rule, the electrode was calibrated before as well as after use, and we detected no change of its sensitivity following the impalements, whether the electrode tip was broken or intact. Tip potentials (defined as the difference in reference electrode signal between isosmotic solutions of NaCl and KCl) ranged from 0 to 15 mV, but electrodes with tip potentials greater than 5 mV were discarded. The response time of the electrodes was less than 2 sec. The two barrels were connected to a high-impedance preamplifier by a pair of silver wires. The signal of the reference barrel was electronically subtracted from the signal of the ion-elective barrel, and the output together with the signal of the reference barrel and the voltage-clamp current were continuously recorded on a multichannel chart recorder (Watanabe MC-611). The intracellular Cl^- activity was calculated by:

$$a_{Cl}^{c} = a_{Cl}^{o} \cdot 10^{\Delta E/S}$$

where a_{Cl}^{o} is the Cl^- activity of the outside bathing Ringer's, ΔE is the differential electrode signal with reference to the outer bath, and S is the sensitivity.

Impalements

Due to the position of the microscope objective, the electrode was advanced at an angle of 25 to 30° relative to the epithelial surface. The electrode was advanced by a hydraulic motorized step micromanipulator (David Kopf Instruments, Model 1207B) with a minimal step length of 0.25 μm.

Often, the initially recorded potential decayed to a much smaller value within a few seconds indicating that the membrane was damaged by the penetration. Penetration of the outermost tough keratinized stratum corneum layer may give rise also to artifactual potentials of the nondecaying type (Nelson et al., 1978). Carefully selected criteria for acceptable impalements are therefore mandatory. The criteria were defined according mainly to Armstrong and Garcia-Diaz (1981) and Zeuthen (1984):

1. Visually the electrode tip should be seen to be localized within a principal cell (a granulosum or, in some experiments, a germinativum cell). However, due to the distortion of the tissue we could not always evaluate whether the cell impaled from the outside belonged to the outermost living epithelial cell layer or to a more deeply located layer.

2. The potential changes should be sudden.

3. During a steady state, the electrode signals should be time invariant. Following perturbations of the transepithelial potential, the electrode signals should return to their initial values when V was stepped back and the initial steady-state re-established.

4. Following impalement, the electrode-resistance (R_e) should be comparable to R_e measured outside the epithelium. Furthermore, R_e should be identical before and after the impalement indicating that the tip is not damaged or blocked.

5. The voltage divider ratio should suddenly increase indicating that a major resistance barrier was passed.

Due to the specific properties of the tissue, another criterium was to be fulfilled for epithelia exposed to NaCl-Ringer's outside: Application of amiloride to the outside bath should result in a hyperpolarization of the reference electrode potential (Nagel, 1976; Helman & Fisher, 1977).

Determination of the Relationship Between I_{Cl} and D_{MRC}

To estimate the density of the m.r. cells we employed the silver-staining technique (Rudneff, 1865; Whitear, 1975). The outside of the skin was rinsed with distilled water. Following 4-min exposure to 0.25% $AgNO_3$, the surface was rinsed again with distilled water and exposed to daylight or artificial light for a few minutes. Following this treatment, the m.r. cells were clearly visible. The density was determined either by direct microscopic counting of m.r. cells in randomly selected areas or by counting within skin areas of 0.5 mm^2 from photographs at 300× magnification. The Cl^- current was determined as the difference between the steady-state voltage-clamp current measured at $V = -100$ mV (mucosal solution negative) and the leak-current, i.e. the voltage-clamp current measured initially after stepping V from 40 to -100 mV.

Measurements of Unidirectional Cl^- Fluxes

Influx and efflux of ^{36}Cl were measured in paired (whole) skins of the same toad mounted in Perspex® chambers with exposed areas of 7 cm^2 according to the method described by Katz and Larsen (1984). Briefly, the skin was bathed with NaCl-Ringer's on the inside and KCl-Ringer's on the outside, and clamped at the desired potential with automatic correction for the resistance between the potential bridges. The current and potential were continuously monitored by a dual pen-recorder and, in addition, the current was time-integrated and read when a sample of the "cold" solution was taken. Starting with 50 mV, each pair of skins was used for measurements of Cl^- fluxes at usually three different clamping potentials. In 10 experiments, V was brought back to 50 mV after having finished the third period, and the measurements continued for a fourth period.

Sign Conventions

The transepithelial potential difference (V) is referenced as the potential of the mucosal bath (ψ_o) minus the potential of the

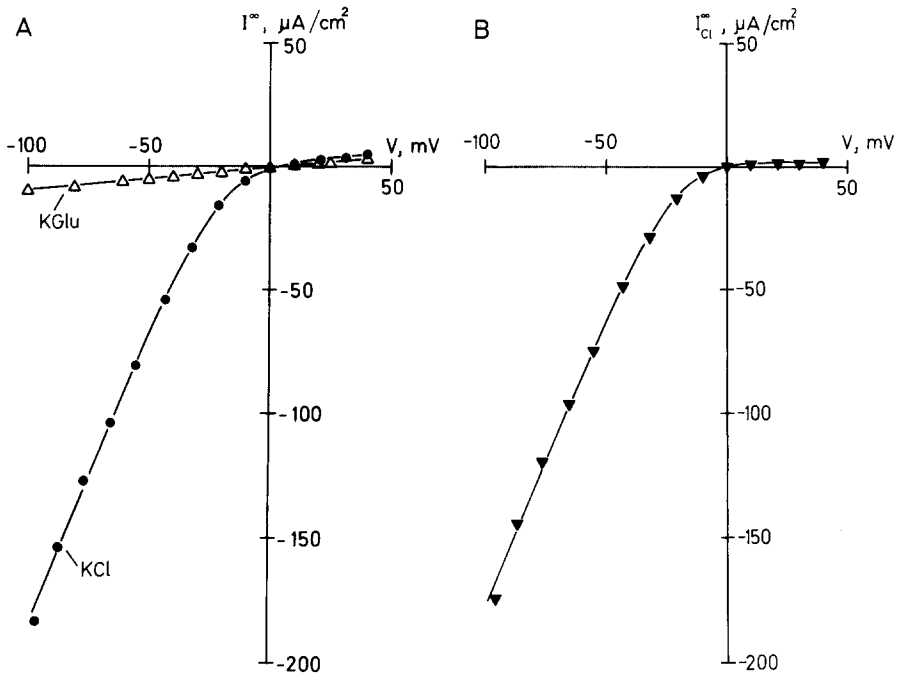

Fig. 2. (*A*) Potential dependence of steady-state currents through toad skin exposed to either KCl Ringer's (●) or K-gluconate Ringer's (△) outside. Inside bath, NaCl-Ringer's. (*B*) Estimated *I–V* relationship of the Cl^--conductive pathway obtained as the difference between the two graphs shown in Fig. 2*A*.

serosal bath (ψ_i), $V = \psi_o - \psi_i$. Intracellular potentials are referenced with respect to the bath from which the micropipette was advanced, i.e. from the apical bath, $V_a = \psi_c - \psi_o$, or from the serosal bath, $V_b = \psi_c - \psi_i$, where ψ_c is the potential of the micropipette with the tip positioned in a cell. Inward currents are defined positive.

Results

Potential Dependence of Transepithelial Currents

Figure 2*A* shows that with Cl^--Ringer's outside, steady-state transepithelial currents were strongly rectified with large outward-going components for $V < 0$ mV. The linear *I/V* relationship of the tissue with gluconate outside reflects a leakage conductance of less than 100 μS/cm². The difference in the currents seen in the two graphs of Fig. 2*A* provides an estimate of the I_{Cl}–*V* relationship of the preparation (Fig. 2*B*). The result indicates that the Cl^- ions are free to flow through the skin for $V < 0$ mV, but not for $V > 0$ mV. The same conclusion was obtained from Cl^- flux measurements in skins exposed to NaCl-Ringer's on the outside (Bruus et al., 1976).

Whereas the above method is fast, and can be applied to a single preparation, a detailed analysis of the conductive pathways requires the measurement of Cl^- influx (J^{in}_{Cl}) and Cl^- outflux (J^{out}_{Cl}) in paired belly skin halves from the same toad. The results are collected in Table 1, and the *I–V* relationships are depicted in Fig. 3*A*. The conclusion to be drawn from the graphs shown in Fig. 3*A* is the same as that suggested by the indirect determination of the I_{Cl}–*V* relationship shown in Fig. 2*B*. The I_{Cl}–*V* relation intersects the I-axis at -1.81 ± 0.31 μA/cm² (mean ± SE, significantly different from zero, $P < 0.05\%$, $n = 11$). Since the Cl^- ions are distributed in electrochemical equilibrium at $V = 0$ mV, this result shows that the Cl^- ions are influenced by a driving force derived from a source other than the electrochemical potential difference of Cl^- between the inner and outer bathing solution. In Fig. 3*B* is shown the relation between the Cl^- current component and the total membrane current. The equation of the regression line is $I = 1.05\ I_{Cl} - 2.19$ μA/cm², which is not significantly different from the line of identity, showing that the outward-clamping currents were carried by an inward flow of Cl^- ions. For $V > 0$ mV, the Cl^- currents were too small to account for the clamping currents which, therefore, were carried by other ions, probably K^+ (*see* Fig. 3*A*).

In ten sets of preparations, clamping at 50 mV finished the experimental protocol of 4-hr duration. In the final flux period, $I_{Cl} = 0.48 \pm 1.96$ μA/cm², as compared to $I_{Cl} = -0.58 \pm 0.73$ μA/cm² for $V = 50$ mV in the initial flux period following mounting of the preparations. Thus, the increase in Cl^- conductance was fully reversible. Furthermore, even in these experiments of long duration nonphysiological Cl^- leaks did not develop.

At $V = 50$ mV, the total membrane current

Table 1. Unidirectional fluxes in toad skin exposed to NaCl-Ringer's on the inside and KCl-Ringer's on the outside[a]

V (mV)	J^{in} (pmol/cm²sec)	J^{out} (pmol/cm²sec)	J^{in}/J^{out} Observed	J^{in}/J^{out} Theoretical	I_{Cl} (μA/cm²)	I_{tot} (μA/cm²)	(n)
50	57 ± 17	51 ± 18	1.48 ± 0.25	0.14	−0.58 ± 0.73	14.2 ± 4.7	(13)
25	70 ± 25	58 ± 23	1.47 ± 0.34	0.37	−1.11 ± 0.99	12.2 ± 10	(5)
0	52 ± 7	33 ± 6	1.64 ± 0.12	1.00	−1.81 ± 0.31	−1.01 ± 0.21	(11)
−25	303 ± 71	76 ± 12	3.88 ± 0.33	2.67	−22.0 ± 5.8	−22.0 ± 4.2	(5)
−50	655 ± 78	67 ± 11	10.6 ± 1.0	7.14	−56 ± 6.7	−55.6 ± 7.5	(8)
−75	1055 ± 131	43 ± 5	24.4 ± 2.1	19.1	−98.0 ± 12	−99.0 ± 12	(7)
−100	1367 ± 222	29 ± 4.5	61.6 ± 13.3	51.0	−129 ± 21	−136 ± 23	(8)
50	128 ± 23	127 ± 30	1.27 ± 0.20	0.14	0.48 ± 1.96	30.1 ± 8.7	(10)

[a] Mean ± SE (number of paired preparations). The theoretical flux-ratios were calculated from (Ussing, 1949), $J^{in}/J^{out} = [Cl]_o/[Cl]_i \exp(-FV/RT)$.

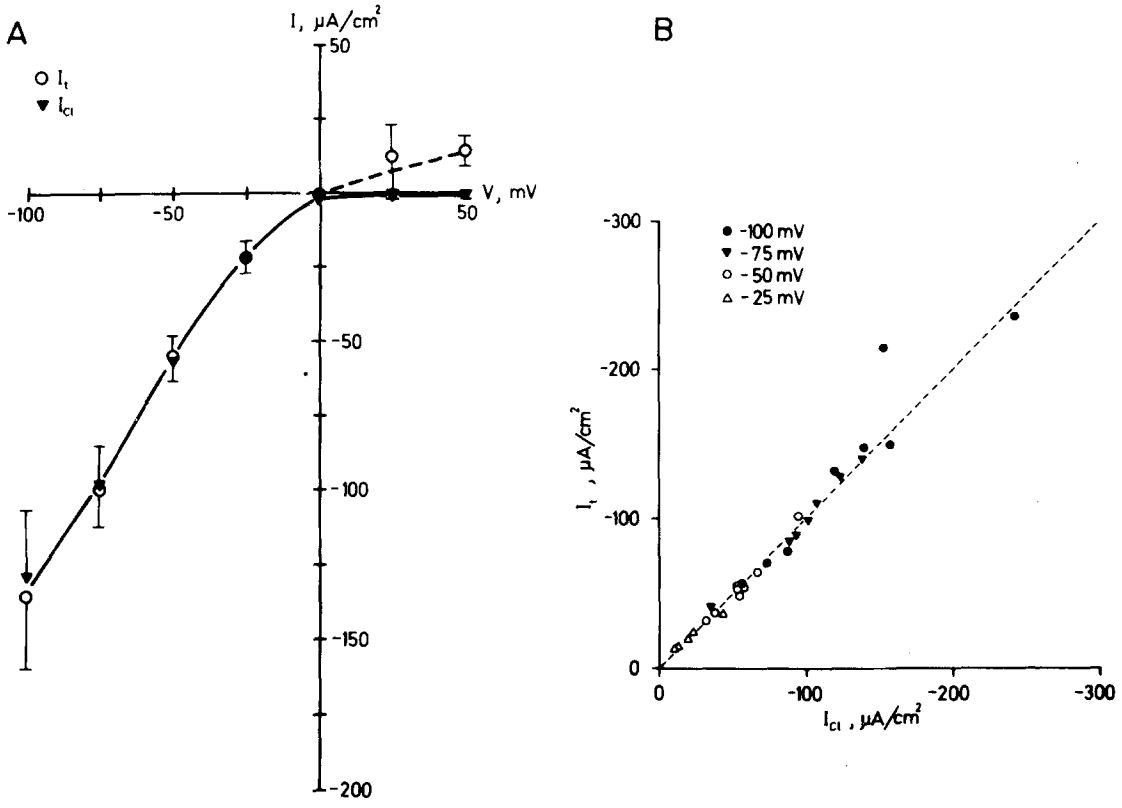

Fig. 3. (*A*) Steady-state current-voltage relationships of toad skin exposed to outside KCl-Ringer's and inside NaCl-Ringer's. The Cl^- currents were estimated from measurements of unidirectional $^{36}Cl^-$ fluxes. (*B*) Relationship between estimated Cl^- currents and clamping currents of toad skin in the negative regions of the current-voltage relationship. The equation of the regression-line is $I_t = 1.05\ I_{Cl} - 2.19\ \mu A/cm^2$ ($n = 28$)

amounted to 14.2 ± 4.7 μA/cm² (initial period) and 30.1 ± 8.7 μA/cm² (final period). It is apparent, therefore, that the cation conductance at $V = 50$ mV became significantly larger towards the end of these experiments characterized by long-duration voltage clamping at positive potentials.

Potential Dependence of the Ratio of Unidirectional Cl^- Fluxes

The asymmetry of the potential dependence of the Cl^- fluxes was further analyzed from the relation between their ratio and potential (*see* Fig. 4). For V

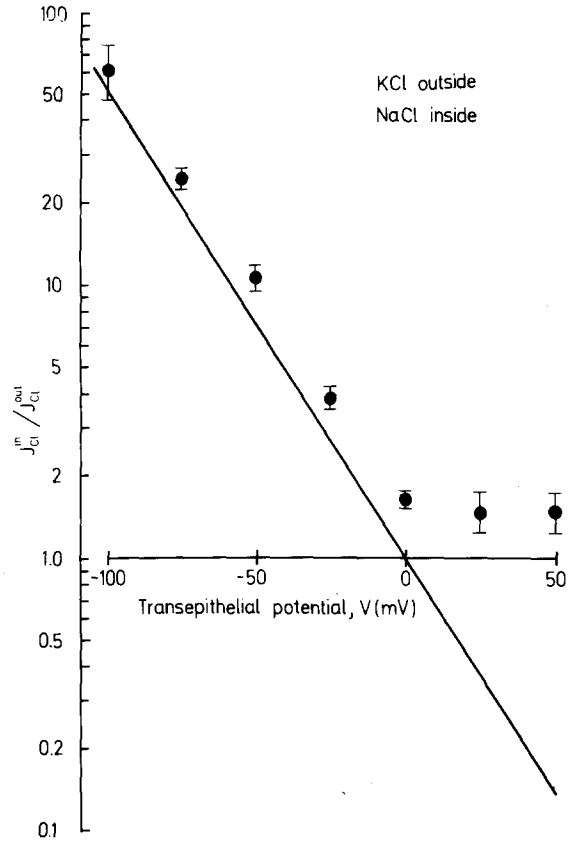

Fig. 4. Dependence of the ratio of unidirectional fluxes on transepithelial potential. The line is drawn according to the theoretical relation for independent fluxes (Ussing, 1949)

> 0 mV, the influx as well as the efflux were largely unaffected by V (Table 1), and the ratios were closer to unity than to the theoretical values for electrodiffusive ion flows. A similar result was obtained with skins exposed to NaCl-Ringer's on both sides (Larsen & Rasmussen, 1982; Dürr & Larsen, 1986) and it strongly indicates that significant components are carried by a 1 : 1 exchange diffusion pathway. In similar agreement with the above studies, the present material reveals an active flux component for $V = 0$ mV, and an electro-diffusive behavior of the fluxes for $V < 0$ mV.

Influence of External Ions on the Time Course of Voltage-Clamp Currents

The results above show that the transepithelial Cl^--conductive pathway is turned off in skins clamped at $0 < V < 50$ mV and is activated in the region of physiological potentials. The time course of the transition from deactivated to the activated state was followed by monitoring the change in clamping current in response to a fast shift of V from 50 to -100 mV. Figure 5, left panel, shows that these currents are dependent on the major anions in the outer bathing solution. In the presence of chloride or bromide, but not gluconate, the current increased slowly to a new steady state, revealing the slow activation of the anion conductance. It is also seen that the process of activation was fully reversible. Figure 5, right panel, shows that the time course of the voltage-clamp currents and their steady-state values were independent of the major cations in the outer bathing solution. Furthermore, as the peak value of the inward current recorded upon return of V to 50 mV was independent of whether Na^+ or choline was present in the outer bath, it is indicated that cations do not pass the voltage-activated pathway.

The above results provide the evidence that the transient currents are carried by Cl^- ions across the external border of the epithelium and that this pathway also is permeable for Br^-, but not for gluconate. [For a more detailed analysis of the anion selectivity of the Cl^- pathway, *see* Harck and Larsen (1986)].

Intracellular Potential and Chloride Activity in Short-Circuited Epithelia

Isolated epithelia from toads adapted to distilled water were impaled from the outside under short-circuit conditions. Figure 6 depicts two impalements of principal cells of a preparation exhibiting a relatively high short-circuit current (40 μA/cm^2). During the first impalement, the recorded intracellular potential was instantaneously -50 mV, but declined to -46 mV within about 100 sec. Within the first 15 to 20 sec of the impalement, a_{Cl}^{ε} approached 23 mM. During the subsequent impalement, the potential initially reached a value of -53 mV and stayed constant for about 100 sec. In this case the intracellular Cl^- activity was 21 mM, i.e. close to the value of the first impalement. With the microelectrode tip in an intracellular position, a brief transepithelial pulse of -100 mV was applied at approximately $t = 350$ sec giving rise to a 100-μA/cm^2 deflection of the clamping current and a 73-mV deflection of the reference electrode signal. From the latter the fractional apical membrane resistance can be calculated: $fR_a = R_a/(R_a + R_b) = \Delta V_a/\Delta V = 0.73$. The a_{Cl}^{ε}-trace is seen to show capacitative transients

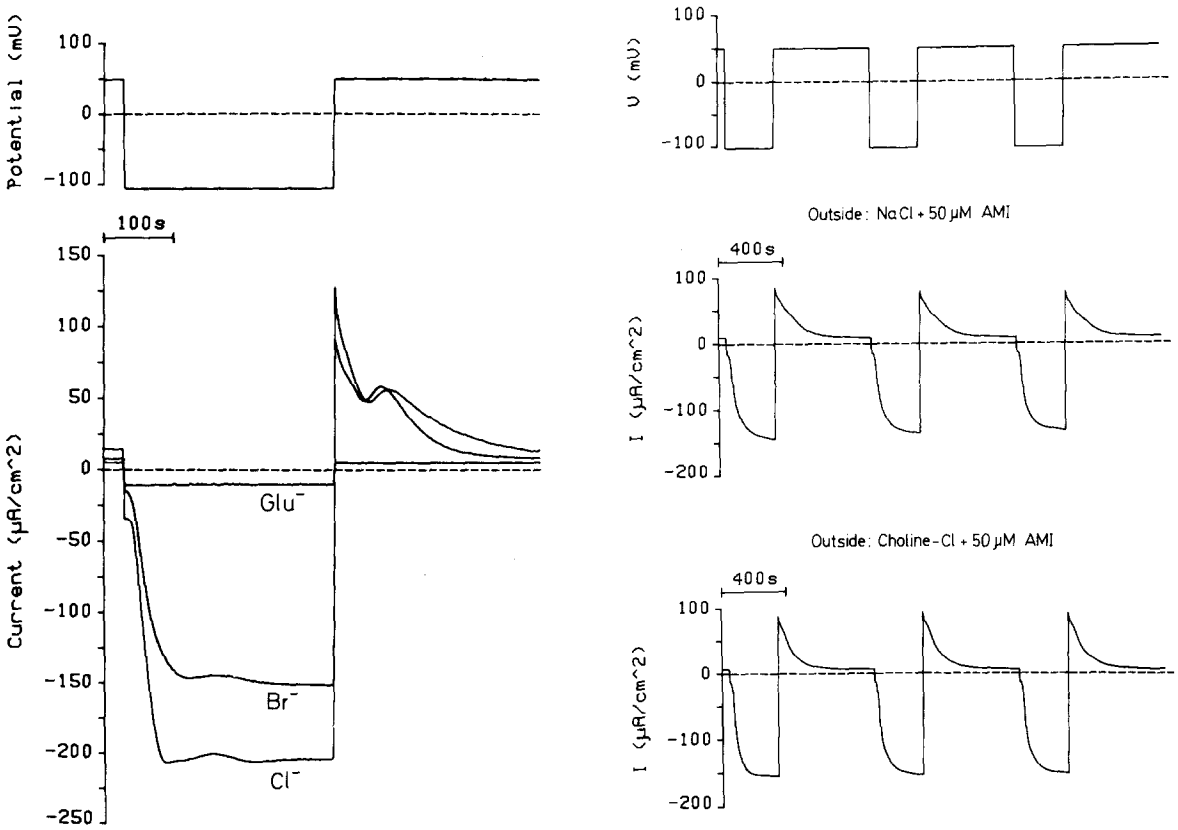

Fig. 5. Left panel: Voltage-clamp currents of toad skin with NaCl-Ringer's inside and KCl Ringer's, KBr-Ringer's or K-gluconate Ringer's outside with the major anions indicated on the graphs. Voltage-clamp program indicated on top. Right panel: As in left panel but with varying cation-composition of the outer bath. The voltage-clamp currents indicate that the time course for the development of the activated Cl^- conductance is independent of the external cations, and that the activation mechanism is not exchausted by repeated activations

in both directions.[2] The intracellular localization of the electrode tip was confirmed by application of 10^{-6} M amiloride to the outer bathing solution leading to a hyperpolarization of V_a by 10 to 25 mV as depicted in Fig. 7. Amiloride treatment led to no change in a^c_{Cl}. Thus, in four preparations (I_{sc} = 19.8 ± 1.8 μA/cm²) a^c_{Cl} was 15.4 ± 3.2 mM and 15.1 ± 2.9 mM before and 25 min after addition of amiloride, respectively.

Table 2 collects the results of 24 impalements from six preparations. It is seen that the values scatter considerably between the preparations but little within a single preparation. Preparations exhibiting large short-circuit currents tend to have numerically smaller intracellular potentials and higher intracellular Cl^- activities. In Fig. 8*A* is shown the relationship between V_a and I_{sc}. These variables were found

Table 2. Short-circuit current, intracellular potential and chloride activity of principal cells from animals adapted to distilled water

Preparation	I_{sc} (μA/cm²)	V_a (mV)	a^c_{Cl} (mM)	n
1	20.0 ± 0.0	−59.0 ± 5.7	16.0 ± 1.9	2
2	24.8 ± 4.4	−54.2 ± 6.4	14.3 ± 1.8	5
3	41.7 ± 2.6	−49.0 ± 3.9	23.4 ± 3.2	6
4	25.8 ± 0.5	−79.5 ± 6.4	17.2 ± 3.9	4
5	17.8 ± 5.6	−95.3 ± 2.1	14.7 ± 2.5	4
6	20.0 ± 0.0	−82.7 ± 4.6	19.6 ± 0.5	3
Mean ± SD	27.0 ± 9.6	−67.9 ± 18.5	18.0 ± 4.4	24
Mean ± SE	27.0 ± 2.0	−67.9 ± 3.8	18.0 ± 0.9	

[2] The much larger capacitance of the resin-filled Cl^--selective barrel results in capacitative current transients following voltage perturbations that are much larger than for the electrolyte-filled reference barrel. Furthermore, as the resistance of the Cl^--selective barrel is more than 100 times larger than that of the reference barrel, the time constant is so large that the slowly relaxing capacitative current is monitored even by the slow-responding pen recorder.

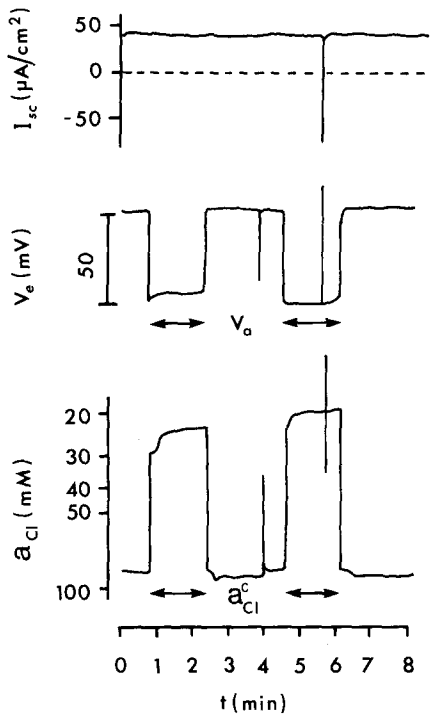

Fig. 6. Impalements of two principal cells in the short-circuited epithelium. The three panels depict the short-circuit current, the intracellular potential, and the difference between the Cl^--selective barrel and the reference barrel signals converted to Cl^- activity. V_e denotes the reference electrode signal. At t = 350 sec V is briefly perturbed by −100 mV. Horizontal arrows indicate periods of intracellular recordings

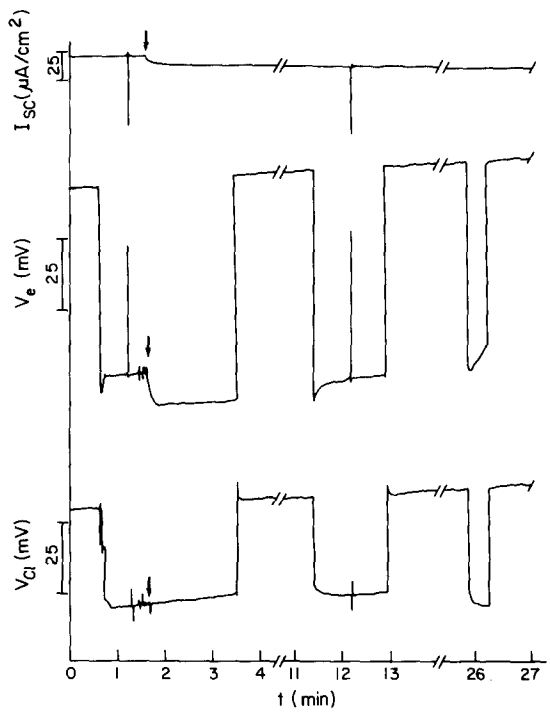

Fig. 7. Effect of amiloride addition (arrows) on short-circuit current, apical membrane potential and intracellular Cl^- activity within half an hour. V_e denotes the reference electrode signal. Amiloride hyperpolarizes the membrane potential, from −64 to −75 mV whereas the Cl^- activity remains constant at 19.5 mM. Ten min after amiloride addition the membrane potential has relaxed to −70 mV. a^c_{Cl} is unchanged. After 25 min V_a is −68 mV and a^c_{Cl} is 15 mM

to be positively correlated with a value of $V_a \simeq -100$ mV for $I_{sc} = 0$ μA/cm^2. A plot of a^c_{Cl} against I_{sc} (Fig. 8*B*) revealed a positive correlation between these variables with $a^c_{Cl} \simeq 9$ mM for $I_{sc} = 0$ μA/cm^2.

Membrane Potentials, Cl^- Activity and Fractional Membrane Resistance During Activation and Deactivation of the Cl^- Conductance

As for the flux-ratio analysis, this series of experiments was conducted with epithelia from animals adapted to a dry milieu with free access to tap water. The epithelium was exposed to KCl-Ringer's on the outside and impaled at a transepithelial clamping potential of 40 mV (mucosa positive) at which the transepithelial Cl^- conductance (G_{Cl}) is deactivated (Table 1, Figs. 2–5). As an example, Fig. 9 depicts an acceptable impalement. After the initial potential deflections caused by the penetration of stratum corneum, a stable electrode signal of about −61 mV, and a fractional outer membrane resistance of 0.71 were obtained. In contrast to the low a^c_{Cl} found in skin from animals adapted to distilled water, epithelia from this group of animals typically showed intracellular Cl^- activities of about 40 mM. In the example shown, a^c_{Cl} was 42 mM. At t = 120 sec, V was stepped to −100 mV resulting in the characteristic sigmoidal increase of the clamping current that is associated with activation of the transepithelial Cl^- conductance (*see* Fig. 5). As the Cl^- activities of the outside and inside bathing solution are identical, the voltage-activated Cl^- conductance can be estimated by $G_{Cl} = \Delta I/V = -88/-100 = 0.88$ mS/cm^2, i.e. a value close to those obtained for whole skins (Table 1). V_a changed instantaneously by 99 mV, to 38 mV, (cell interior positive with respect to the mucosal bath). During the following 90 sec, V_a changed only slightly. Except for a brief capacitative transient, the signal from the Cl^--selective electrode remained unchanged, indicating that a^c_{Cl} stayed constant in spite of the large increase of the transepithelial Cl^- conductance. Within the following 90 sec, no significant change of a^c_{Cl} occurred. At t = 220 sec, V was returned to 40 mV resulting in an instantaneous reversal of the clamping current that, in turn, slowly relaxed to its pre-

Table 3. Intracellular parameters of toad skin epithelium during activation and deactivation of transepithelial chloride conductance (G_{Cl}); KCl-Ringer's outside mean ± SE; n = 15

Transepithelial potential, V	V_a (mV)	a^c_{Cl} (mM)	fR_a	G_{Cl}(mS/cm²)[a]
40 mV, G_{Cl} deactivated	−70.1 ± 5.0	40.0 ± 3.8		
−100 mV before activation of G_{Cl}	31.3 ± 5.6	42.3 ± 4.3	0.69 ± 0.03	
−100 mV after activation of G_{Cl}	27.1 ± 6.4	41.4 ± 4.3		1.19 ± 0.10
40 mV before deactivation of G_{Cl}	−67.8 ± 3.9	38.9 ± 4.4	0.67 ± 0.03	

[a] G_{Cl} was determined as the difference in the transepithelial conductance measured at −100 and 40 mV, respectively.

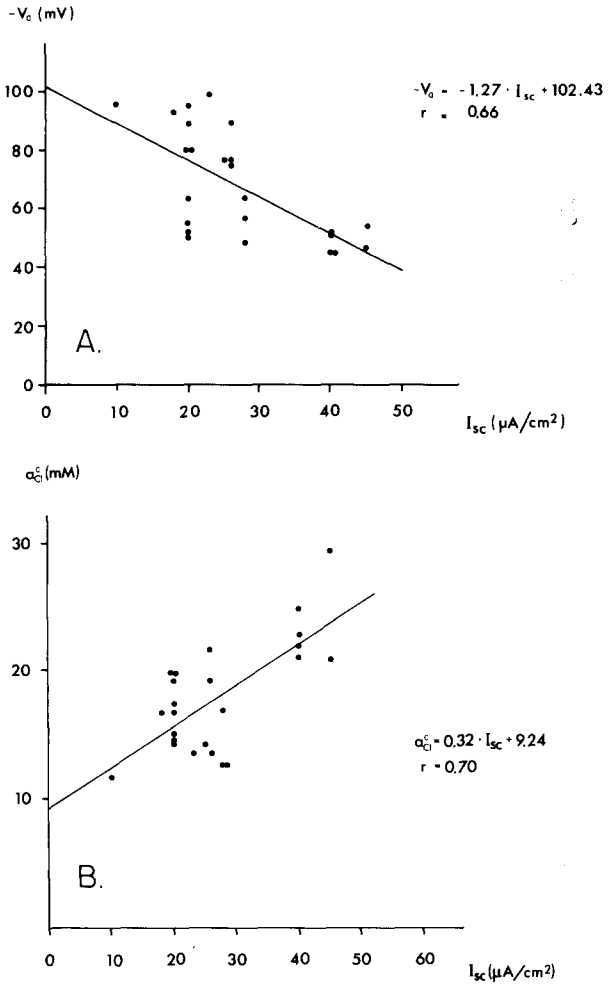

Fig. 8. (*A*) Relation between the intracellular potential under short-circuit conditions and the short-circuit current. The regression line is given by $-V_a = -1.27 \times I_{sc} + 102.43$ ($r = 0.66$). (*B*) Relationship between intracellular Cl^- activity and short-circuit current. The regression line is given by $a^c_{Cl} = 0.32 \times I_{sc} + 9.24$ ($r = 0.70$)

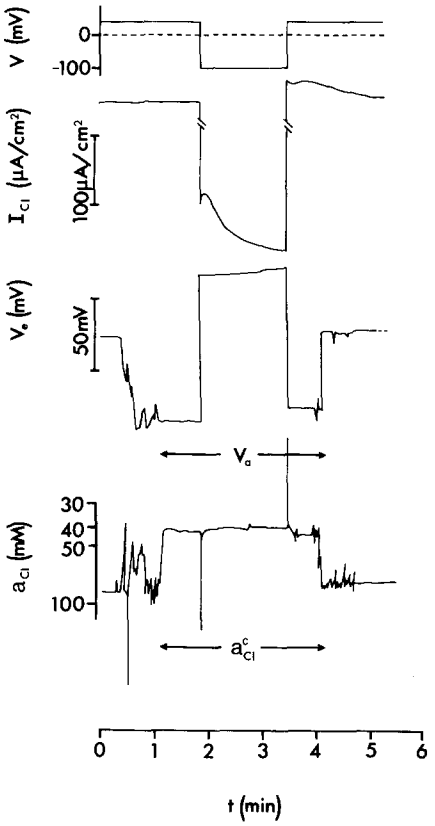

Fig. 9. Simultaneous recordings of the voltage-clamped transepithelial potential, the short-circuit current, the apical membrane potential (V_e denotes reference electrode signal) and the intracellular Cl^- activity during activation and deactivation of the transepithelial Cl^- conductance by shifting V from 40 to −100 mV, and back

pulse steady-state value, illustrating that the conductance activation was fully reversible. The reference electrode potential instantaneously returned to a value slightly less than that prior to the G_{Cl} activation, and remained constant. The Cl^- electrode potential again exhibited a capacitative deflection, but remained thereafter constant at a slightly depolarized value. After 30 sec, the electrode was withdrawn and both electrode potentials returned to values close to their original baseline values. In Table 3 is shown the mean values of V_a, a^c_{Cl}, fR_a and the increase of G_{Cl} from 15 impale-

Table 4. Basolateral membrane potential, fractional membrane resistance and intracellular Cl^- activity of the principal cells at deactivated and activated G_{Cl}; impalements from the inside

V_b(40 mV) (mV)	V_b(−100 mV) (mV)	ΔV_b (mV)	fR_b	fR_a	a^c_{Cl} (mM)
−34	−91	−57	0.41	0.59	36
−45	−90	−45	0.32	0.68	28
−40	−75	−35	0.26	0.74	33
−56	−91	−35	0.26	0.74	32
−62	−99	−37	0.26	0.74	26
−45	−90	−45	0.32	0.68	32
−55	−82	−27	0.19	0.81	32
−18	−45	−27	0.19	0.81	32
−26	−44	−18	0.15	0.85	30
−21	−45	−24	0.17	0.83	31
−40.2 ± 4.8[a]	−75.2 ± 7.0	−35.0 ± 3.7	0.25 ± 0.03	0.75 ± 0.03	31.2 ± 0.9

[a] Mean ± SE; n = 10.

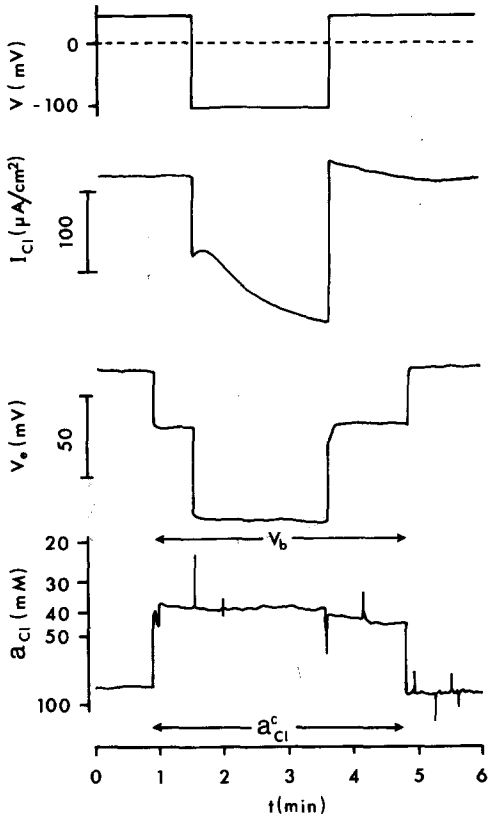

Fig. 10. Impalement of a stratum germinativum cell from the inside. Same protocol as in Fig. 9

ments. It can be seen that the imposed change of the transepithelial potential from 40 to −100 mV instantaneously shifted V_a by 101.4 mV from −70.1 ± 5.0 mV to 31.3 ± 5.6 mV. During the next 2 to 5 min, while G_{Cl} became nearly maximally activated, V_a did not change significantly ($P > 0.1$). Likewise, a^c_{Cl} stayed constant ($P > 0.1$) irrespective of whether G_{Cl} was deactivated (40 mV) or nearly maximally activated (new steady state at −100 mV). Also fR_a was independent of the transepithelial conductance (0.67 compared to 0.69). Returning V to 40 mV resulted in an instantaneous shift in V_a by 94.9 to −67.8, mV which is not significantly different from V_a recorded before stepping the transepithelial potential to −100 mV.

As the cells are impaled from the outside bath, the microelectrode is advanced through the cornified layer of cells. This leads to a significant distortion of the epithelium that might have influenced the conductive properties of the cell membranes. In another series of experiments, therefore, the epithelium was impaled from the serosal side. Figure 10 depicts an impalement fulfilling our criteria. At t = 60 sec the cell was impaled and the basolateral membrane potential (V_b) was found to be −34 mV. The intracellular Cl^- activity was 38 mM, i.e. close to the value determined from impalements from the outside. After approximately 40 sec the clamping potential was shifted from 40 to −100 mV causing a hyperpolarization of V_b by −57 to −91 mV. The difference signal of the two barrels varied but little, indicating that a^c_{Cl} remained almost constant during the transition of the epithelium to a new steady state. After about 120 sec, G_{Cl} was nearly maximally activated and V was stepped back to 40 mV, which led to a return of V_b to −34 mV. During the following minute, V_b remained constant whereas a^c_{Cl} increased somewhat. However, following electrode withdrawal it was seen that also the baseline for the Cl^--selective electrode signal had changed a comparable amount, indicating that the intracellular Cl^- activity, also in this case, changed but little during the sequence of Cl^- conductance activation/deactivation. Qualitatively, the observed behavior of V_b and a^c_{Cl} is in agreement with that observed during impalements from the outside. Table 4 summarizes the results of 10 impalements. It is seen that the

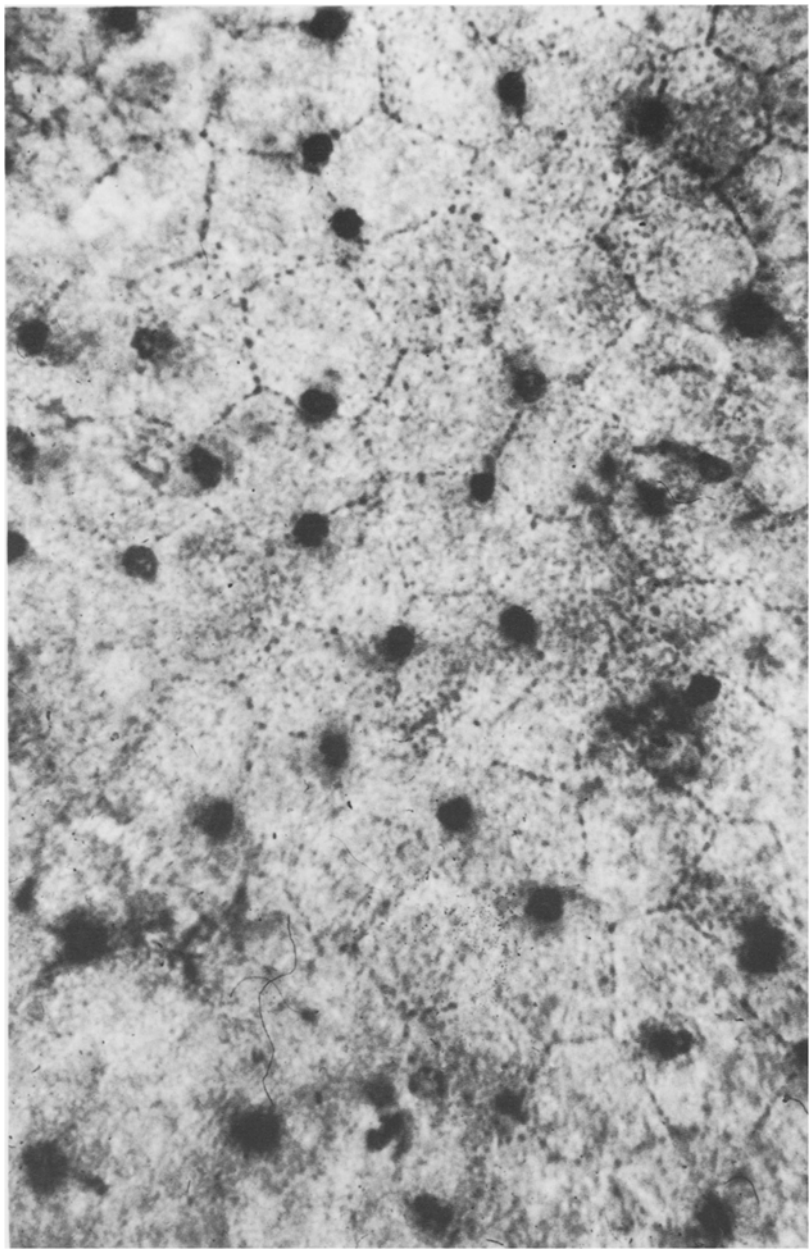

Fig. 11. Ag^+-stained toad skin epithelium. Mitochondria-rich cells are clearly visible. Note the small surface area of the m.r. cells compared to the granulosum cells

observed potential profiles determined by impalement from the outside and inside, respectively, are quantitatively in agreement. However, a^c_{Cl} was found to be somewhat lower, 31.2 mM, in the germinativum cells.

Ag^+ Staining of the Mitochondria-Rich Cells

Due to their small size and scattered distribution beneath the cornified cells it was not possible for us to impale the m.r. cells. Additionally, they were pushed out of focus as the micropipettes were advanced through the stratum corneum. Therefore we chose another experimental approach for investigating their possible role in transepithelial Cl^- transport. These cells have for long been known to be selectively stained by silver ions (Rudneff, 1865). Ag^+ is also known to stain selectively the apical crypt of the fish gill chloride cells (Philpott, 1965), and the chloride cells of the fish opercular membrane (our own *unpublished observations*). Recently, the latter cell type was shown to secrete Cl^- ions (Scheffey et al., 1983). The Ag^+ staining mechanism is believed to reflect the precipitation of AgCl directly outside the membrane areas having a significant Cl^- permeability. Besides the m.r. cells,

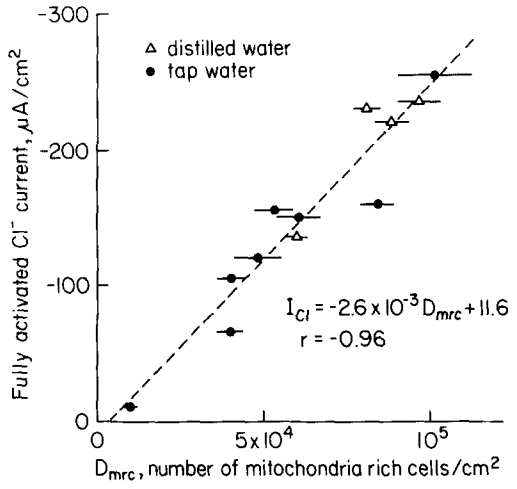

Fig. 12. Relationship between the current through the fully activated Cl^- conductance ($V = -100$ mV) and the density of m.r. cells. Each point indicates the mean D_{MRC} observed in animals adapted to tap water (●) or distilled water (△). The regression line is given by $I_{Cl} = -2.6 \times 10^{-3} \times D_{MRC} + 11.6$ ($r = -0.96$)

the tight junction areas were also found to be slightly stained (Fig. 11). Probably, this reflects the nonselective increase of the paracellular permeability due to Ag^+ exposure reported from frog skin (Curran, 1972) and corneal epithelium (Klyce & Marshall, 1982). In six experiments in which the skins prior to Ag^+ exposure had been bathed on both sides with Cl^--free Ringer's for 2 hr, we found no silver staining of the m.r. cells. The staining method itself, thereby, indicates that the apical membrane of the m.r. cells is permeable to Cl^- ions, whereas the apical membrane of the outermost principal cells is not.

In skins from 12 animals adapted to either tap water or distilled water we determined the density of m.r. cells (D_{MRC}) and the Cl^- current flowing through the fully activated chloride conductance at -100 mV. A linear correlation between these parameters (Fig. 12), characterized by a correlation coefficient of -0.96 and a slope of -2.5 nA per m.r. cell, was found. Both D_{MRC} and the Cl^- current of skins adapted to distilled water was generally higher than those from skins adapted to tap water.

Discussion

Components of the Transepithelial Cl^- Fluxes

The potential dependence of the Cl^- current (Fig. 3) and of the Cl^- flux ratio (Fig. 4) reveal different modes of Cl^- transport through the toad skin bathed with KCl-Ringer's on the outside. Thus, at potentials above 0 mV the net flux of Cl^- was not significantly different from zero in spite of a measurable tissue conductance reflected in the I–V relation shown in Fig. 3*A*. These steady-state currents, observed under conditions of no Cl^- net flux are most likely carried by K^+ through the principal cells (Zeiske & Van Driessche, 1979; Nagel & Hirschmann, 1980; Van Driessche & Zeiske, 1980), and the Cl^- fluxes are most likely carried by a Cl/Cl exchange transport system.

The active Cl^- component, revealed at $V = 0$ mV, is of a small magnitude, $I_{Cl} = -1.8 \pm 0.31$ μA/cm^2, but it is equal to the value of the short-circuited frog skin bathed with choline-Ringer's outside, $I_{Cl} = -2.6 \pm 1.2$ μA/cm^2 (Drewnowska & Biber, 1985), and short-circuited toad skin exposed to NaCl-Ringer's with 50 μM amiloride on the outside, $I_{Cl} = -1.6 \pm 0.3$ μA/cm^2 (Dürr & Larsen, 1986). All of these values are smaller than the active Cl^- currents in short-circuited skins exposed to bilateral NaCl-Ringer's, $I_{Cl} = -5.2 \pm 1.5$ μA/cm^2 (toad skin, Bruus et al., 1976), and $I_{Cl} = -12.3 \pm 3.1$ μA/cm^2 (frog skin, Drewnowska & Biber, 1985). The above studies provide additional examples that active Cl^- transport can occur in the isolated short-circuited amphibian skin, as first demonstrated by Zadunaisky and co-workers (Zadunaisky et al., 1963). A possible dependence of the active Cl^- flux on active transport of Na^+ was discussed by Harvey and Kernan (1984), Drewnowska and Biber (1985), and Biber et al. (1985) and they suggested that an electroneutral transport system is localized to the apical membrane of the outermost principal cell layer (for further discussion, *see below*).

In the physiological range of potentials ($V < 0$ mV), the activated Cl^- conductance directed the total current across the epithelium (Fig. 3). The flux-ratio analysis indicated that these large currents are predominantly passive (Fig. 4), in agreement with the result of previous studies with skins exposed to bilateral NaCl-Ringer's (Larsen & Rasmussen, 1982; Kristensen, 1983; Dürr & Larsen, 1986) or to 1/10 NaCl-Ringer's on the outside (Koefoed-Johnsen et al., 1952*a*). This conclusion is also in agreement with the low temperature coefficient (Q_{10}) of these currents; in nine preparations, Q_{10} ranged from 1.1 to 1.5 (Willumsen & Larsen, 1982).

Apical Membrane Potential in Steady State

Intracellular potentials of amphibian skin have been reported during the last three decades. As discussed by Nagel (1979) studies until 1975 often reported small intracellular potentials (-10 mV $< V_a < -40$ mV) under short-circuit conditions, and trans-

epithelial potential profiles of the staircase type under open-circuit conditions. Selection of microelectrodes with small tip-diameter (for discussion, *see* Nelson et al., 1978) and establishment of more strict criteria for acceptance of measurements (Nagel, 1976; Helman & Fisher, 1977) has led to considerably increased values of reported intracellular potentials. Thus, Nagel (1975, 1977) and Helman and Fisher (1977) concordantly reported V_a values in the order of −100 mV under short-circuit conditions and a well-type potential profile under open-circuit conditions. Since then it has been generally accepted that V_a on the average is somewhere between −60 and −80 mV (Nagel, 1976; Nagel et al., 1981; Giraldez & Ferreira, 1984). However, typically a broad interval of V_a values is reported in each study, (Nagel, 1976; Garcia-Diaz et al., 1985). Nagel (1976), for instance, reports 67 measurements in the interval $-113\ \text{mV} < V_a < -32\ \text{mV}$ with a mean value of −73 mV in frog skin exposed to NaCl-Ringer's on both sides. In the present study, we found V_a values in the interval $-98\ \text{mV} < V_a < -45$ mV and a mean of −67.9 mV. Among epithelia of different animals the mean V_a varied from −95.3 to −49.0 mV (Table 2). Only little variation of membrane potentials was seen among cells of the individual preparations.

The variation of V_a was found to be correlated with the short-circuit current as was also found by Nagel (1976). Animals having large I_{sc} exhibited small intracellular potentials and vice versa (Fig. 8*A*). This relationship most likely reflects that variation in I_{sc} is caused by a variation of the apical membrane Na^+ permeability. Accordingly, the intercept of −100 mV (Fig. 8*A*) is a measure of the K^+ equilibrium potential giving an intracellular K^+ concentration $K_c = K_i \cdot \exp(-FE_K/RT) \simeq 2.4 \cdot \exp(-96{,}500 \times (-0.1)/(8.31 \times 295)) = 123$ mM, in reasonably good agreement with values reported from electron microprobe studies of toad skin (Rick et al., 1980). In agreement with this notion, as P^a_{Na} was decreased by adding 10^{-4} M amiloride to the mucosal bath, V_a hyperpolarized by 10 to 25 mV (Fig. 7) as reported by others (Nagel et al., 1981; Garcia-Diaz et al., 1985).

With KCl-Ringer's on the outside, and V clamped to 40 mV (mucosa positive) we recorded, on the average, an apical membrane potential of -71 ± 5 and -80 ± 5 mV by impalements from the outside and the inside, respectively. This reveals a mean basolateral membrane potential of −31 and −40 mV, respectively, i.e. significantly smaller than the estimated V_b with NaCl outside. Most likely, these small values of V_b reflect a reduced inner membrane K^+ permeability, whereby the membrane potential is driven towards the equilibrium potentials of the two other diffusible ions (Na^+ and Cl^-). Support for this interpretation comes from a recent study by Davis and Finn (1982) showing that in the toad urinary bladder reduction of the Na^+ conductance (amiloride) of the apical membrane leads to a decrease of the K^+ conductance of the basolateral membrane, whereby the cells become depolarized.

Intracellular Cl^- Activity Under Short-Circuit Conditions

Under short-circuit conditions the mean a^c_{Cl} was found to be 18 mM in skins from toads adapted to distilled water. This pretreatment is known to stimulate the passive transepithelial Cl^- conductance (Fig. 12, Katz & Larsen, 1984). The value for a^c_{Cl}, which is equivalent to an intracellular Cl^- concentration of 23 mM if the cell Cl^- activity coefficient equals that in free solution (0.76), is in agreement with those of other microelectrode studies (Nagel et al., 1981; Giraldez & Ferreira, 1984; Harvey & Kernan, 1984), but far below the values measured by other techniques, for instance wash-out experiments (Ferreira & Ferreira, 1981; Stoddard & Helman, 1982) and electron microprobe analyses (Rick et al., 1978, 1980; Dörge et al., 1985), which lead to intracellular concentrations in the order of 40 to 50 mM. Table 5 summarizes a^c_{Cl} determinations from the literature. The reason for the discrepancy between the two groups of methods is at present unknown. The discrepancy becomes even larger if, as shown by Spring and Kimura (1978) and McCaig and Leader (1984), the Cl^- activities measured with liquid ion exchanger (Orion) microelectrodes should be corrected for a value of approximately 4 to 6 mM due to interfering cytoplasmic anions (e.g. bicarbonate, acetate, propionate, and isethionate). No major Cl^- pool seems to be physically or chemically compartmentalized within the cells as a total exchangeable Cl^- pool of 40 to 50 mM was shown to be osmotically active (MacRobbie & Ussing, 1961; Ussing, 1985). However, all estimates of a^c_{Cl} yield values far above the equilibrium activity. Employing the measured V_a value of −68 mV, the theoretical thermodynamic intracellular equilibrium activity is calculated to be approximately 5.5 mM. Based on this observation, together with the demonstration of a low apical membrane Cl^- permeability (Ferreira & Ferreira, 1981) and the responses of cell volume (Ussing, 1982) and a^c_{Cl} (Dörge et al., 1985) to furosemide or bumetanide in the inner bath, the existence of a basolateral NaCl cotransport system in the principal cells was suggested. The cotransport system which is supposedly equivalent to the type described from other cell types, for instance gallbladder (Frizzell et al., 1979) and Ehrlich ascites tu-

Table 5. Intracellular chloride activities and concentrations reported from amphibian skin

Reference	Species	a_{Cl}(mM)	c_{Cl}(mM)	n	Conditions[a]	Method
MacRobbie & Ussing (1961)	*R. temporaria*		49 ± 2	6	o.c.	Osmotic method
Ussing (1985)	*R. temporaria*		41		o.c.	
Nagel et al. (1981)	*R. pipiens*	18 ± 3		5	s.c.	Ionselective
Giraldez & Ferreira (1984)	*R. ridibunda*	21.9 ± 1.5		5	s.c.	Ionselective
Harvey & Kernan (1984)	*R. temporaria*	20.3 ± 1.6		60	o.c.	microelectrodes
Biber et al. (1985)	*R. pipiens*	15.5 ± 0.5		102	s.c.	
Present study	*B. bufo*	18.0 ± 4.4		24	s.c.	
Present study	*B. bufo*	40.0 ± 3.8		15	V = 40 mV	
Present study	*B. bufo*	31.2 ± 0.9[b]		10	V = 40 mV	
Zylber et al. (1973)	*L. ocellatus*		57.2 ± 5.3	11	i.c.	Chemical analysis
Ferreria & Ferreira (1981)	*R. ridibunda*		47.0 ± 2.9 to 59.8 ± 3.8	10 8	s.c.	Washout experiments
Stoddard & Helman (1982)	*R. pipiens*		42		s.c.	
Rick et al. (1978)	*R. temporaria* *R. esculenta*		48 ± 7[c]	19	s.c.	Electron microprobe analysis[f]
Rick et al. (1980)	*B. viridis*		52 ± 6[d]	27	s.c.	
Dörge et al. (1985)	*R. temporaria*		51 ± 3[e]	>20		

[a] o.c. = open circuit, s.c. = short circuit, i.c. = isolated cells.
[b] Germinativum cells impaled from the basolateral side.
[c] 36.5 ± 5.0 mmol/kg wet mass.
[d] 39.9 ± 4.9 mmol/kg wet mass.
[e] 39.1 ± 2.7 mmol/kg wet mass (mean ± 2 SEM).
[f] The electron microprobe values are multiplied by 1.3 (conf. references) in order to express the concentration as mmol/liter cell water volume.

mor cells (Hoffmann et al., 1983), transports electrically silent Na^+, K^+ and $2Cl^-$ (Geck et al., 1980) from the serosal compartment into the principal cell compartment driven by the Na^+ gradient across the basolateral membrane (Ussing, 1985).

The observed correlation at steady state, between a^c_{Cl} and I_{sc} (r = 0.70) (Fig. 3*B*) is in accordance with the findings of Harvey and Kernan (1984). The interdependence of the intracellular Cl^- activity and the short-circuit current is not intuitively comprehended from the above theory, because the intracellular potential (V_c) and Na^+ activity (a^c_{Na}) may change with the apical membrane Na^+ permeability (the short-circuit current). We expect, therefore, that the passive (depending on V_c) as well as the active (depending on a^c_{Na}) Cl^- flux components across the basolateral membrane have new values at different steady states.

Membrane Potential and Cl^- Activity do not Reflect the Dynamics of G_{Cl}

In the short-circuited frog skin amiloride inhibits the active Na^+ transport, and reduces the unidirectional Cl^- fluxes, as well (Candia, 1978; Kristensen, 1978). A similar reduction of the Cl^- fluxes was observed in response to substitution of external Na^+ by a nonpermeating cation (Macey & Meyers, 1963; Kristensen, 1978; Ques-von Petery et al., 1978). These observations indicate that the transepithelial Cl^- fluxes take a transcellular route and that the cells involved take part in the active Na^+ transport.

The principal cells, which constitute the major cell population of the epithelium, are responsible for the active amiloride-inhibitable Na^+ transport and, therefore, meet a necessary requirement of being the Cl^- transporting cell type mentioned above. However, our experiments show that the fractional apical membrane resistance of these cells which is of the same size as reported by others (e.g., Nagel et al., 1981) does not change significantly within a period of 2 to 5 min following a 140-mV shift in the clamped transepithelial potential, despite the fact that G_{Cl} in the same period of time increases by 1.19 mS/cm^2 (from the deactivated to the fully activated state). If, for instance, a major voltage-dependent Cl^- conductance residing in the apical membrane of the principal cells was responsible for the observed increase in the transepithelial Cl^- conductance this increase would be paralleled by a significant reduction of fR_a.

Table 6. Cellular chloride activity, membrane potentials, electrochemical Cl^- potential differences and driving forces across the membranes of the principal cells during activation of the transepithelial Cl^- conductance in toad skin

Transepithelial potential, V (mV)	a^c_{Cl}* (mM)	$V_a = \psi_c - \psi_o$* (mV)	$V_b = \psi_c - \psi_i$ (mV)	$\Delta\tilde{\mu}^a_{Cl}$†	$\Delta\tilde{\mu}^b_{Cl}$ (Joule/mole)	$\Delta\tilde{\mu}^a_{Cl}/-F$	$\Delta\tilde{\mu}^b_{Cl}/-F$ (mv)
+40	40 ± 4	−71 ± 3	−31 ± 3	5033	−1173	−52	12
−100 before activation of G_{Cl}	42 ± 4	31 ± 5	−67 ± 5	−4884	−4766	51	49
−100 after activation of G_{Cl}	41 ± 4	29 ± 6	−71 ± 6	−4557	−5093	47	53

* Mean ± SE; $n = 15$.

† $\Delta\tilde{\mu}^a_{Cl} = \tilde{\mu}^c_{Cl} - \tilde{\mu}^o_{Cl} = RT\ln(a^c_{Cl}/a^a_{Cl}) - F(\psi_c - \psi_o)$; $\Delta\tilde{\mu}^b_{Cl} = \tilde{\mu}^i_{Cl} - \tilde{\mu}^c_{Cl} = RT\ln(a^i_{Cl}/a^c_{Cl}) - F(\psi_i - \psi_c)$; $R = 8.31\ J \cdot mol^{-1} \cdot K^{-1}$; $T = 295$ K; $F = 96{,}500$ Coul · eqv.$^{-1}$; $a^i_{Cl} = a^o_{Cl} = 0.74 \times 113$ mM = 84 mM (Ringer's solution).

Furthermore, the finding of an a^c_{Cl} far above that of passive distribution suggests active accumulation of Cl^- ions in the principal cell compartment with small dissipative Cl^- permeabilities of the cell membranes. We estimated the passive driving force for Cl^- ion flow across the apical and the basolateral membrane at $V = 40$ mV and $V = -100$ mV, respectively. The driving force was calculated by $-\Delta\tilde{\mu}/F$, where $\Delta\tilde{\mu}$ is the estimated difference in electrochemical potential for Cl^- across the membrane and F is the Faraday. It is seen (Table 6) that shifting V from 40 to −100 mV resulted in a change of the driving force across the apical membrane from −52 mV (outward direction) to 51 mV (inward direction). The driving force across the basolateral membrane changed from 12 to 49 mV (both being directed from cell to serosal bath). Despite these considerable changes of the driving force for Cl^- flow no change in a^c_{Cl} was seen during the transition to a new steady state, suggesting low Cl^- permeabilities of both membranes. In agreement with the observations of Nagel et al. (1981) and Dörge et al. (1985) we find that exposure of the short-circuited skin to amiloride does not change a^c_{Cl} significantly within half an hour despite the subsequent hyperpolarization of V_a that causes an increased driving force for Cl^- flow out of the cells. A small apical membrane Cl^- permeability was also suggested by Biber et al., 1985, who found that the intracellular Cl^- activity of the short-circuited frog skin did not drop in the absence of mucosal Cl^- ions. The relatively large P_{Cl} of the basolateral membrane reported by Ferreira and Ferreira (1981) and Giraldez and Ferreira (1984) from washout experiments using Cl^--free inner solutions might reflect Cl^- leaving the cellular compartment by the cotransport system as a consequence of the reversed gradient for Cl^- across the basolateral membrane. Recently, Stoddard et al. (1985) have reported large, fairly symmetrical and electrically silent Cl^- fluxes across the basolateral membrane of the frog skin. These fluxes, that were inhibited by furosemide and SITS (4-acetamido-4′-isothiocyanostilbene-2,2′-disulfonic acid) were concluded to result from either a Cl^-/Cl^- or a Cl^-/HCO_3^- exchange mechanism. The presence of such a Cl^- transport system would not necessarily lead to changes in a^c_{Cl} in response to a change in the potential profile and is therefore not in contradiction with the conclusion of our study. Thus, the lack of change in a^c_{Cl} in answer to large perturbations of the electrical gradients across the membranes adds further evidence against the hypothesis of a major electrodiffusive Cl^- transport pathway being located in the principal cells.

Under certain conditions, for instance when the skin is stimulated by epinephrine (Koefoed-Johnsen et al., 1952*a*) or isoproterenol (Thompson & Mills, 1983), the skin glands are involved in an outward-directed active Cl^- transport. However, the voltage-dependent Cl^- pathway cannot be localized to the cells of the skin glands which are embedded deeply into the subepithelial connective tissue, the corium, as the isolated epithelium retains the Cl^--transporting characteristics of the intact skin despite the fact that both the mucous glands and the poison glands are normally left in the corium when the epithelium is isolated by collagenase treatment (Carasso et al., 1971).

Localization of the Voltage-Dependent G_{Cl}

Two lines of experimental evidence lead to the hypothesis that the Cl^- fluxes pass through the mitochondria-rich cells. Exposure of the apical side to amiloride, or substitution of external Na^+ by a nonpermeant cation inhibit the unidirectional Cl^- fluxes through the short-circuited skin. Theoretical treatments (Candia, 1978; Kristensen, 1982) predict that the intracellular hyperpolarization associated with elimination of the apical membrane Na^+ conductance, result in a significant decrease of unidirectional equilibrium Cl^- fluxes through the cell. Conversely, activation of the Na^+ conductance of the apical membrane of an epithelial cell that is permeable for Cl^- ion flow, is predicted to result in increased equilibrium Cl^- fluxes under short-circuit

Table 7. Densities of mitochondria-rich cells (D_{MRC}) of amphibian skin epithelia

Reference	$D_{MRC}(cm^{-2})$	Species
Whitear (1975)	213.600[a]	*R. temporaria*
Brown et al. (1981)	37.000–198.000[b]	*R. temporaria*
	134.000–232.000[c]	*X. laevis*
Eskesen (*unpublished*)	2.000–180.000[d]	*R. temporaria*
Present study	9.900–100.600[d]	*B. bufo*

[a] Estimated from plate *I* (*a*) of the paper.
[b] Dorsal and abdominal D_{MRC}, respectively.
[c] Abdominal and dorsal D_{MRC}, respectively.
[d] Total range observed.

conditions. Kristensen (1981) studied the Cl^- efflux in the short-circuited frog skin in the presence of, respectively, BIG (benzimidazolylguanidine) and AVT (arginine vasotocin) which both are known to activate the Na^+ permeability (Ussing & Zerahn, 1951; Fuchs et al., 1977; Nagel, 1978; Li et al., 1982). However, it was found that only BIG stimulates the Cl^- flux. As the principal cells are AVT sensitive (Nagel, 1978), Kristensen concluded that the Cl^- ions pass a BIG-sensitive, Na^+-transporting cellular pathway which is parallel to the principal cells, and he suggested that these cells are the mitochondria-rich cells.

Voûte & Meier (1978) studied the Cl^- influxes in frog skins exposed to Cl^--free Ringer's on the inside. The active Na^+ transport was eliminated with either amiloride or KCl Ringer's on the outside. Under these conditions it was found that the Cl^- current was proportional to the number of m.r. cells per mm of sections of 1-μm thickness. Furthermore, these investigators found that the m.r. cells, but not the principal cells, swelled following exposure of the skin to K-gluconate on the inside and KCl on the outside indicating that the apical membrane of the m.r. cells, only, is permeable to Cl^-.

The results of the present study show that the Cl^- current through the fully activated Cl^- conductance (measured at $V = -100$ mV) is linearly correlated to the density of m.r. cells (Fig. 12). The relation between D_{MCR} and I_{Cl} was found to be $I_{Cl} = -2.6 \times 10^{-3} D_{MRC} + 11.6$. D_{MRC} is a highly variable parameter, as seen from Table 7, which quotes some values from the literature. It is seen that D_{MRC} varies among individuals of the same species, as well as among different species. Also, it is apparent that D_{MRC} varies between different skin areas of a single animal, for instance between dorsal and abdominal skin areas. Further, recently D_{MRC} has been shown to be dependent on the salinity to which the animal has been adapted (Katz & Larsen, 1984).

Due to the small contribution of the m.r. cells to the total epithelial surface and the large observed I_{Cl} through the maximally activated Cl^- conductance, our results indicate that the apical membranes of the m.r. cells possess a very high passive Cl^- conductance. Considering a mean I_{Cl} per m.r. cell of -2.6 nA (the slope of the observed relation between I_{Cl} and D_{MRC}) we arrive at a conductance of about 200 mS per cm^2 surface area of mitochondria-rich cell. This impressive figure compares with the Cl^- conductance of 580 mS/cm^2 of the Cl^- cells of teleosts (Foskett et al., 1983) and with the peak Na^+ conductance of about 750 mS/cm^2 at the node of frog myelinated axon (Hille, 1984). However, due to the presence of microvilli (Whitear, 1975) on the apical membrane, the specific conductance of the apical membrane of m.r. cells might be an order of magnitude lower.

We are grateful to Dr. T. Zeuthen for his advice and for supplying equipment for the microelectrode measurements. Also we would like to thank Dr. R.C. Boucher for useful discussions and Mrs. Lis Christensen and Sharon Womble for excellent typing of the manuscript. We also want to thank Dr. Karen Eskesen for allowing quotation of unpublished observations. N.J. Willumsen was supported by the Danish Natural Science Research Council, grants 11-3086, 11-3624 and 11-4222, and equipment was purchased by grants DNSRC 11-4374 and 11-4670.

References

Armstrong, W. McD., Garcia-Diaz, J.F. 1981. Criteria for the use of microelectrodes to measure membrane potentials in epithelial cells. *In:* Epithelial Ion and Water Transport. A.D.C. Macknight and L.P. Leader, editors. pp. 43–53. Raven, New York

Biber, T.U.L., Drewnowska, K., Baumgarten, C.M., Fisher, R.S. 1985. Intracellular Cl activity changes of frog skin. *Am. J. Physiol.* **249:**F432–F438

Brown, D., Grosso, A., De Sousa, R.C. 1981. The amphibian epidermis: Distribution of mitochondria-rich cells and the effect of oxytocin. *J. Cell. Sci.* **52:**197–213

Bruus, K., Kristensen, P., Larsen, E.H. 1976. Pathways for chloride and sodium transport across toad skin. *Acta Physiol. Scand.* **97:**31–47

Candia, O.A. 1978. Reduction of chloride fluxes by amiloride across the short-circuited frog skin. *Am. J. Physiol.* **234:**F437–F445

Carasso, N., Favard, P., Jard, S., Rajerison, R.M. 1971. The isolated frog skin epithelium. I. Preparation and general structure in different physiological states. *J. Microscopie* **10:**315–330

Curran, P.F. 1972. Effect of silver ion on permeability of frog skin. *Biochim. Biophys. Acta* **288:**90–97

Davis, C.W., Finn, A.L. 1982. Sodium transport inhibition by amiloride reduces basolateral membrane potassium conductance in tight epithelia. *Science* **216:**525–527

Dörge, A., Rick, R., Beck, F., Thurau, K. 1985. Cl transport across the basolateral membrane in frog skin epithelium. *Pfluegers Arch.* **405:**S8–S11

Drewnowska, K., Biber, T.U.L. 1985. Active transport and ex-

change diffusion of Cl across the isolated skin of *Rana pipiens*. *Am. J. Physiol.* **249:**F424–431

Dürr, J.E., Larsen, E.H. 1986. Indacrinone (MK-196)—A specific inhibitor of the voltage dependent Cl^- permeability in toad skin. *Acta Physiol. Scand.* **127:**145–153

Ehrenfeld, J., Masoni, A., Garcia-Romeu, F. 1976. Mitochondria-rich cells of frog skin in transport mechanisms: Morphological and kinetic studies on transepithelial excretion of methylene blue. *Am. J. Physiol.* **231:**120–126

Ferreira, K.T.G., Ferreira, H.G. 1981. The regulation of volume and ion composition in frog skin. *Biochim. Biophys. Acta* **646:**193–202

Foskett, K.J., Bern, H.A., Machen, T.E., Conner, M. 1983. Chloride cells and the hormonal control of teleost fish osmoregulation. *J. Exp. Biol.* **106:**255–281

Frizzell, R.A., Field, M., Schultz, S.G. 1979. Sodium-coupled chloride transport by epithelial tissues. *Am. J. Physiol.* **236:**F1–F8

Fuchs, W., Larsen, E.H., Lindemann, B. 1977. Current-voltage curve of sodium channels and concentrations dependence of sodium permeability in frog skin. *J. Physiol. (London)* **267:**137–166

Garcia-Diaz, J.F., Baxendale, L.M., Klemperer, G., Essig, A. 1985. Cell K activity in frog skin in the presence and absence of cell current. *J. Membrane Biol.* **85:**143–158

Geck, P., Pietrzyk, C., Burckhardt, B.C., Pfeiffer, B., Heinz, E. 1980. Electrically silent cotransport of Na^+, K^+, Cl^- in Ehrlich cells. *Biochim. Biophys. Acta* **600:**432–447

Giraldez, F., Ferreira, K.T.G. 1984. Intracellular chloride activity and membrane potential in stripped frog skin (*Rana temporaria*). *Biochim. Biophys. Acta* **769:**625–628

Harck, A., Larsen, E.H. 1986. Concentration dependence of halide fluxes and selectivity of the anion pathway in toad skin. *Acta Physiol. Scand.* **128:**289–304

Harvey, B.J., Kernan, R.P. 1984. Intracellular ion activities in frog skin in relation to external sodium and effects of amiloride and/or ouabain. *J. Physiol. (London)* **349:**501–517

Helman, S.I., Fisher, R.S. 1977. Microelectrode studies of the active Na transport pathway of frog skin. *J. Gen. Physiol.* **69:**571–604

Hille, B. 1984. Ionic channels of excitable membranes. pp. 1–426. Sinauer Associates, Sunderland, Massachusetts

Hoffman, E.K., Sjøholm, C., Simonsen, L.O. 1983. Na^+, Cl^- cotransport in Ehrlich ascites tumor cells activated during volume regulation (regulatory volume increase). *J. Membrane Biol.* **76:**269–280

Katz, U., Larsen, E.H. 1984. Chloride transport in toad skin (*Bufo viridis*). The effect of salt adaptation. *J. Exp. Biol.* **109:**353–372

Klyce, S.D., Marshall, W.S. 1982. Effects of Ag^+ on ion transport by the corneal epithelium of the rabbit. *J. Membrane Biol.* **66:**133–144

Koefoed-Johnsen, V., Levi, H., Ussing, H.H. 1952*a*. The mode of passage of chloride ions through the isolated frog skin. *Acta Physiol. Scand.* **25:**150–163

Koefoed-Johnsen, V., Ussing, H.H., Zerahn, K. 1952*b*. The origin of the short-circuit current in the adrenaline stimulated frog skin. *Acta Physiol. Scand.* **27:**38–48

Kristensen, P. 1978. Effect of amiloride on chloride transport across amphibian epithelia. *J. Membrane Biol.* **Special Issue:**167–185

Kristensen, P. 1981. Is chloride transfer in frog skin localized to a special cell type? *Acta Physiol. Scand.* **113:**123–124

Kristensen, P. 1982. Chloride transport in frog skin. *In:* Chloride Transport in Biological Membranes. J.A. Zadunaisky, editor. pp. 319–332. Academic, New York

Kristensen, P. 1983. Exchange diffusion, electrodiffusion, and rectification in the chloride transport pathway of frog skin. *J. Membrane Biol.* **72:**141–151

Larsen, E.H., Kristensen, P. 1978. Properties of a conductive cellular chloride pathway in the skin of the toad (*Bufo bufo*). *Acta Physiol. Scand.* **102:**1–21

Larsen, E.H., Rasmussen, B.E. 1982. Chloride channels in toad skin. *Philos. Trans. R. Soc. London B* **299:**413–434

Li, J.H.-Y., Palmer, L.G., Edelman, I.S., Lindemann, B. 1982. The role of sodium-channel density in the natriferic response of the toad urinary bladder to an antidiuretic hormone. *J. Membrane Biol.* **64:**77–89

Macey, R.I., Meyers, S. 1963. Dependence of chloride permeability on sodium in the isolated frog skin. *Am. J. Physiol.* **204:**1095–1099

MacRobbie, E.A.C., Ussing, H.H. 1961. Osmotic behaviour of the epithelial cells of frog skin. *Acta Physiol. Scand.* **53:**348–365

McCaig, D., Leader, J.P. 1984. Intracellular chloride activity in Extensor Digitorum Longus (EDL) muscle of the rat. *J. Membrane Biol.* **81:**9–17

Nagel, W. 1975. Intracellular PD of frog skin epithelium. *Pfluegers Arch.* **355:**R70

Nagel, W. 1976. The intracellular electrical potential profile of the frog skin epithelium. *Pfluegers Arch.* **365:**135–143

Nagel, W. 1977. The dependence of the electrical potentials across the membranes of the frog skin upon the concentration of sodium in the mucosal medium. *J. Physiol. (London)* **269:**777–796

Nagel, W. 1978. Effects of antidiuretic hormone upon electrical potential and resistance of apical and basolateral membranes of frog skin. *J. Membrane Biol.* **42:**99–122

Nagel, W. 1979. Microelectrode artifacts and frog skin potentials. (*Letters to the editor*) *J. Membrane Biol.* **51:**97–100

Nagel, W., Garcia-Diaz, J.F., Armstrong, W.McD. 1981. Intracellular ionic activities in frog skin. *J. Membrane Biol.* **61:**127–134

Nagel, W., Hirschmann, W. 1980. K^+-permeability of the outer border of the frog skin (*R. temporaria*). *J. Membrane Biol.* **52:**107–113

Nelson, D.J., Ehrenfeld, J., Lindemann, B. 1978. Volume changes and potential artifacts of epithelial cells of frog skin following impalement with microelectrodes filled with 3 M KCl. *J. Membrane Biol.* **Special Issue:**91–119

Philpott, C.W. 1965. Halide localization in the teleost chloride cell and it's identification by selected area electron diffraction. Direct evidence supporting an osmoregulatory function for the seawater adapted chloride cell of *Fundulus*. *Protoplasma* **60:**7–23

Ques-von Petery, M.V., Rotunno, C.A., Cereijido, M. 1978. Studies on chloride permeability in the skin of *Leptodactylus ocellatus:* I. Na^+ and Cl^- effect on passive movements of Cl^-. *J. Membrane Biol.* **42:**317–330

Rick, R., Dörge, A., Arnim, E. von, Thurau, K. 1978. Electron microprobe analysis of frog skin epithelium: Evidence for a syncytial sodium transport compartment. *J. Membrane Biol.* **39:**313–331

Rick, R., Dörge, A., Katz, U., Bauer, R., Thurau, K. 1980. The osmotic behaviour of toad skin epithelium (*Bufo viridis*). *Pfluegers Arch.* **385:**1–10

Rudneff, M. 1865. Uber die epidermoidale Schicht der Froschhaut. *Arch. Mikrosk. Anat.* **1:**295–298

Scheffey, C., Foskett, J.K., Machen, T.E. 1983. Localization of ionic pathways in the teleost opercular membrane by extracellular recording with a vibrating probe. *J. Membrane Biol.* **75:**193–203

Spring, K.R., Kimura, G. 1978. Chloride reabsorption by renal proximal tubules of *Necturus*. *J. Membrane Biol.* **38:**233–254

Stoddard, J.S., Helman, S.I. 1982. Chloride efflux from isolated epithelia of frog skin. *Fed. Proc.* **41:**1496

Stoddard, J.S., Jakobsson, E., Helman, S.I. 1985. Basolateral membrane chloride transport in isolated epithelia of frog skin. *Am. J. Physiol.* **249:**C318–C329

Thompson, I.G., Mills, J.W. 1983. Chloride transport in glands of frog skin. *Am. J. Physiol.* **244:**C221–C226

Ussing, H.H. 1949. The distinction by means of tracers between active transport and diffusion. *Acta Physiol. Scand.* **19:**43–56

Ussing, H.H. 1982. Volume regulation of frog skin epithelium. *Acta Physiol. Scand.* **114:**363–369

Ussing, H.H. 1985. Volume regulation and basolateral co-transport of sodium, potassium, and chloride ions in frog skin epithelium. *Pfluegers Arch.* **405:**S2–S7

Ussing, H.H., Zerahn, K. 1951. Active transport of sodium as the source of electric current in the short-circuited isolated frog skin. *Acta Physiol. Scand.* **23:**109–127

Van Driessche, W., Zeiske, W. 1980. Ba^{2+}-induced conductance fluctuations of spontaneously fluctuating K^+ channels in the apical membrane of frog skin (*Rana temporaria*). *J. Membrane Biol.* **56:**31–42

Voûte, C.L., Meier, W. 1978. The mitochondria-rich cell of frog skin as hormone-sensitive "shunt path." *J. Membrane Biol.* **Special Issue:**151–165

Whitear, M. 1975. Flask cells and epidermal dynamics in frog skin. *J. Zool. (London)* **175:**107–149

Willumsen, N.J., Larsen, E.H. 1982. Time- and voltage-characteristics of a passive Cl^- pathway in the isolated skin of *Bufo bufo*. *Acta Physiol. Scand.* **114:**28A

Willumsen, N., Larsen, E.H. 1984. Passive chloride transport of the toad skin does not pass through granular cells. *Acta Physiol. Scand.* **120:**46A

Willumsen, N.J., Larsen, E.H. 1985*a*. Membrane potentials and Cl^- activity of the granulosum cells in toad skin in relation to activation/deactivation of the transepithelial voltage sensitive Cl^- conductance. *Acta Physiol. Scand.* **124-**Suppl. 542:156

Willumsen, N.J., Larsen, E.H. 1985*b*. Passive Cl^- currents in toad skin: Potential dependence and relation to mitochondria-rich cell density. *In:* Transport Processes, Iono- and Osmoregulation. R. Gilles and M. Gilles-Baillien, editors. pp. 20–30. Springer, Berlin-Heidelberg

Zadunaisky, J.A., Candia, O.A., Chiarandini, D.J. 1963. The origin of the short-circuit current in the isolated skin of the South American frog *Leptodactylus ocellatus*. *J. Gen. Physiol.* **47:**393–402

Zeiske, W., Van Driessche, W. 1979. Saturable K^+ pathway across the outer border of frog skin (*Rana temporaria*): Kinetics and inhibition by Cs^+ and other cations. *J. Membrane Biol.* **47:**77–96

Zeuthen, T. 1984. The electrophysiology of ion and water transport in gallbladder and other leaky epithelia. D.Sc. Thesis, University of Copenhagen

Zeuthen, T., Hiam, R.C., Silver, I.A. 1974. Recording of ion activities in the brain. *In:* Ion Selective Microelectrodes. H. Berman and N. Herbert, editors. pp. 145–156. Plenum, London

Zylber, E.A., Rotunno, C.A., Cereijido, M. 1973. Ion and water balance in isolated epithelial cells of the abdominal skin of the frog *Leptodactylus ocellatus*. *J. Membrane Biol.* **13:**199–216

Received 31 January 1986; revised 7 July 1986